

Crystal Structure and Functional Analysis of the HERG Potassium Channel N Terminus: A Eukaryotic PAS Domain

João H. Morais Cabral,* Alice Lee,*
Steven L. Cohen,† Brian T. Chait,† Min Li,§
and Roderick Mackinnon*^{||}

*Laboratory of Molecular Neurobiology
and Biophysics

†Laboratory of Mass Spectrometry
and Gaseous Ion Chemistry

‡Howard Hughes Medical Institute
Rockefeller University
New York, New York 10021

§Department of Physiology
The Johns Hopkins University
School of Medicine
Baltimore, Maryland 21205

Summary

The HERG voltage-dependent K⁺ channel plays a role in cardiac electrical excitability, and when defective, it underlies one form of the long QT syndrome. We have determined the crystal structure of the HERG K⁺ channel N-terminal domain and studied its role as a modifier of gating using electrophysiological methods. The domain is similar in structure to a bacterial light sensor photoactive yellow protein and provides the first three-dimensional model of a eukaryotic PAS domain. Scanning mutagenesis of the domain surface has allowed the identification of a hydrophobic “hot spot” forming a putative interface with the body of the K⁺ channel to which it tightly binds. The presence of the domain attached to the channel slows the rate of deactivation. Given the roles of PAS domains in biology, we propose that the HERG N-terminal domain has a regulatory function.

Introduction

HERG (human *eag*-related gene) is a member of the *eag* (*ether-a-go-go*) K⁺ channel family (Warmke et al., 1991; Warmke and Ganetzky, 1994). These channels, found in human heart and nervous system, underlie one form of the long QT syndrome, LQT2 (Curran et al., 1995), a genetic condition causing familial cardiac arrhythmia and sudden death. In common with other voltage-dependent K⁺ channels, HERG has a subunit topology of six membrane-spanning stretches (Figure 1A). Four of these subunits form a tetramer with a central ion conduction pore. Voltage-dependent gating, or opening and closing of the pore, is conferred by the S4 “voltage sensor” (the arginine-rich fourth membrane-spanning stretch) present in all members of the voltage-dependent cation channel family (Sigworth, 1994).

HERG exhibits two distinct and physiologically significant gating characteristics: rapid inactivation and slow deactivation (Trudeau et al., 1995; Smith et al., 1996;

Spector et al., 1996). The presence of rapid inactivation means that when the channel is opened with cell membrane depolarization it very quickly enters a nonconducting (inactivated) state, passing very little current in the outward direction (Figure 1B). When the membrane is returned to its normal resting potential near –80 mV, the channel apparently retraces its conformational steps and passes through the open state on the way back to its closed configuration. The return to the closed state, referred to as the process of deactivation, is very slow in the HERG channel, and consequently a large inward “tail” K⁺ current is observed during a voltage clamp experiment (Figure 1B). This slow rate of HERG channel deactivation plays an important role in cardiac electrical excitability by governing the length of the action potential (Sanguinetti et al., 1995).

Deletion of the HERG cytoplasmic amino terminus has been shown to profoundly affect the rate of deactivation (Schönherr and Heinemann, 1996; Spector et al., 1996; Terlau et al., 1997). This finding is very interesting because the amino terminus of HERG contains a sequence of about 135 amino acids, which is not only highly conserved, but is sufficiently unique to be considered a defining feature of the *eag* K⁺ channel family (Warmke and Ganetzky, 1994). What structural unit is encoded by these amino acids, and why have they been conserved? To address these questions, we have solved the structure of the *eag* N-terminal domain (*eag* domain) by X-ray crystallography and have begun to characterize its interaction with the K⁺ channel using site-directed mutagenesis and electrophysiology. The *eag* domain controls deactivation by tightly associating with the body of the K⁺ channel, presumably through a hydrophobic patch on its surface. Its three-dimensional structure defines the first eukaryotic member of the PAS domain family. PAS (acronym for the gene products of *Per*, *Arnt*, and *Sim*) (Reppert, 1998; Sassone-Corsi, 1998) domains are found in proteins involved in the circadian rhythm, the cyclic patterns of hormone secretion, breeding, and locomotor activity in mammals and the oscillation of photosynthesis in plants. In prokaryotic cells, PAS domains regulate a variety of biochemical processes by serving as light and chemical sensors.

Results

Function of the *eag* Domain

The HERG potassium channel has a ~390 residue cytosolic N terminus, of which the first 135 form the *eag* domain. It was previously shown that removal of the *eag* domain results in active K⁺ channels with altered gating properties (Schönherr and Heinemann, 1996; Spector et al., 1996; Terlau et al., 1997). Electrophysiological recordings from *Xenopus* oocytes injected with RNA encoding wild-type or *eag* domain-deleted HERG (truncated HERG) channels are shown in Figures 2A and 2B. The records focus on the tail currents where the deactivation process (transition back to the closed state) is observed. The deactivation rate is increased markedly

^{||} To whom correspondence should be addressed (e-mail: mackinn@rockvax.rockefeller.edu).

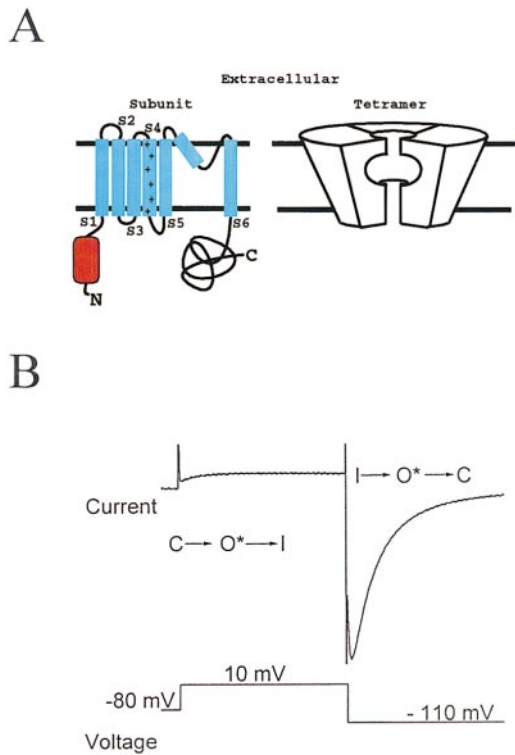


Figure 1. Membrane-Spanning Topology and Current Recorded from HERG K⁺ Channels

(A) The HERG channel monomer has six transmembrane segments (blue) labeled S1 to S6; S4 is the voltage sensor, and it contains six positively charged amino acids as indicated by the + symbols. The channel has a large C terminus and the characteristic N-terminal eag domain (red), both cytosolic; the pore region is situated between S5 and S6. The functional channel is a tetramer with a central ion conduction pathway.

(B) Upon depolarization of the cell membrane to 10 mV from a holding voltage of -80 mV, the channels activate, passing from the closed state C to the open state O* (the * symbol indicates a conducting state) and ionic current is observed in the outward direction. Only a small amount of current is observed because the channels quickly enter the I (inactivated) state, which does not conduct ions. When the membrane is repolarized to -110 mV, the channels pass from the I state to the open state O* and a large inward "tail" current is recorded. This current slowly decays with an increasing number of channels deactivating or returning to the closed state C.

through removal of the eag domain. A double exponential function was fitted to the decay phase of the current traces, and the time constant for the faster, dominant component was graphed as a function of membrane voltage (Figure 2C). The truncated channel exhibits a faster rate of deactivation over voltages studied.

We next asked whether it was possible to reconstitute the wild-type function by application of eag domain produced in *E. coli* (Li et al., 1997) to the cytoplasmic surface of truncated HERG channels. The experiment was carried out in two ways. First, purified domain (corresponding to amino acids 1 to 135 of HERG) was applied at micromolar concentrations to an excised membrane patch containing many truncated HERG K⁺ channels. The domain had no effect on channel gating in this acute exposure experiment (not shown). However, when the

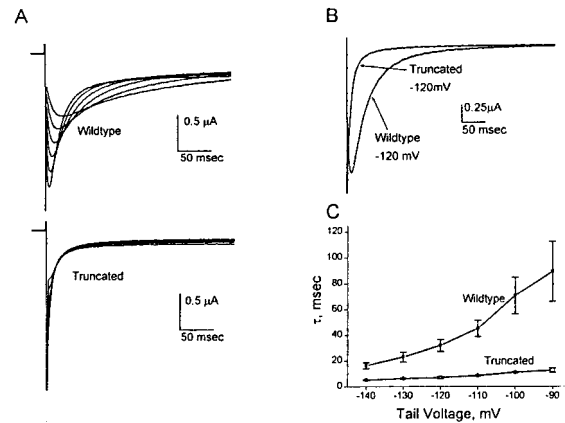


Figure 2. Deactivation of Wild-Type and eag Domain-Deleted (Truncated HERG) Channels

(A) After depolarization to 20 mV (not shown), tail currents for wild-type and truncated HERG channels were elicited by repolarizing the membrane to voltages between -140 mV and -90 mV in 10 mV increments.

(B) Currents recorded as in (A) at -120 mV, scaled to have nearly equal amplitudes, are superimposed.

(C) Plot of deactivation time constant as a function of the repolarization voltage. The time constant is that of the dominant fraction of a double exponential fit to the decay phase of the tail current. Error bars are standard error of the mean (n = 3 - 5).

eag domain protein was instead injected into oocytes expressing truncated HERG, the deactivation kinetics slowly converted to be wild-type-like (Figures 3A and 3B). Within 3 hr, the time constant for deactivation at -110 mV became two times slower, and further slowing progressed over 24 hr. Excision of membrane patches containing "wild-type-reconstituted" HERG showed no speeding of deactivation over a 3 min period (not shown); a rapid change in the deactivation rate upon excision would have been expected if the domain were loosely attached and exerted its effect by rapidly associating and dissociating with the channel. We therefore conclude that the eag domain must be bound tightly to the body of the channel.

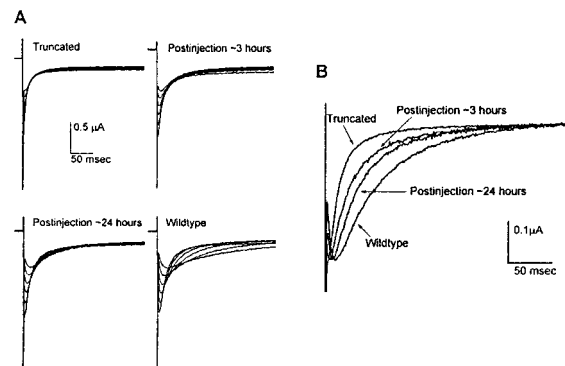


Figure 3. The eag Domain Confers Wild-Type Gating Properties

(A) Tail currents were recorded from oocytes expressing truncated HERG channels 3 and 24 hr after protein injection of eag domain protein. Currents from wild-type and truncated HERG are shown for comparison. The voltage protocol used is the same as in Figure 2A. (B) Scaled currents recorded at -110 mV are superimposed.

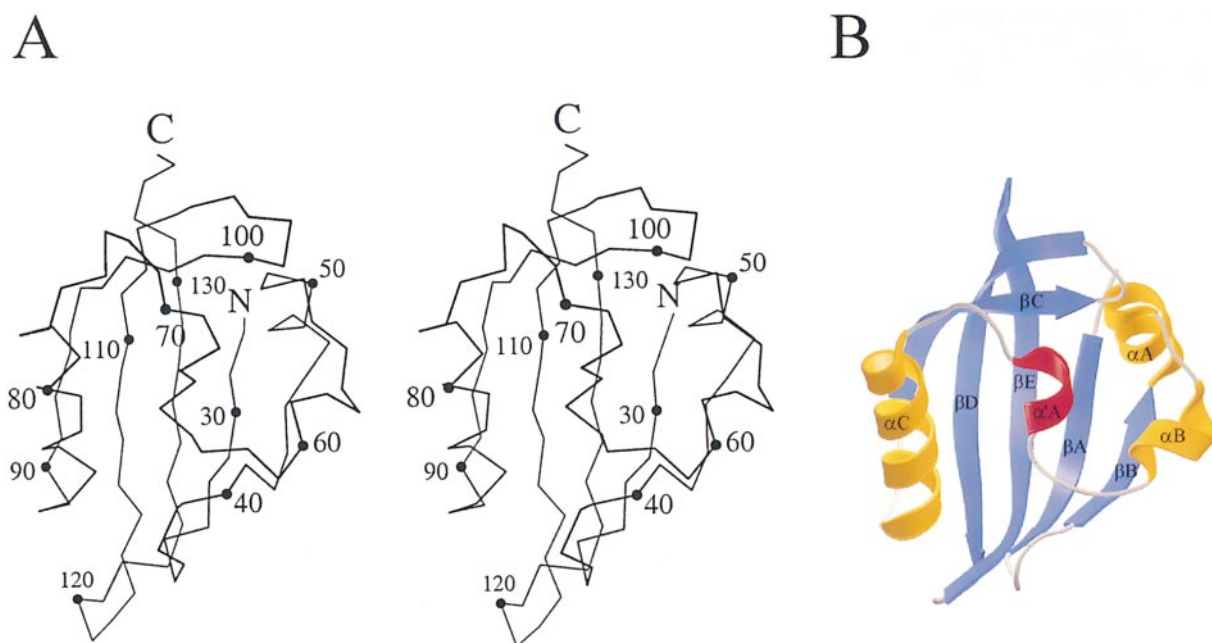


Figure 4. Stereo and Ribbon Diagrams of the eag Domain Three-Dimensional Model

(A) Stereo C α plot with every tenth residue numbered and the N and C termini indicated.

(B) Ribbon diagram with secondary structure elements labeled. These pictures were drawn with MOLSCRIPT (Kraulis, 1991) and RASTER3D (Bacon and Anderson, 1988).

One possible explanation for the effect of the eag domain on the deactivation kinetics is that it could be catalytic, modifying the channel or an effector of the channel already present in the cytoplasm. This indirect mechanism was tested by injecting eag domain into oocytes expressing a full-length channel containing a point mutation (F29A) within its own eag domain. This mutant channel deactivates at a rate that is intermediate between wild-type and truncated HERG, presumably because the F29A mutation renders the domain partially defective (see below). Injected eag domain did not slow deactivation. In other words, it did not compensate for the F29A mutant domain. The most likely explanation is that the mutated domain prevents attachment of the wild-type domain to the channel. This result reinforces the conclusion that the injected eag domain exerts its effect on gating by attaching tightly to the body of the HERG K⁺ channel.

Crystal Structure

The structure of the eag domain was determined by a MAD (multiwavelength anomalous diffraction) experiment with selenomethionine substituted protein crystals at the CHESS F2 beamline. A three-dimensional model consisting of amino acids 26 to 135 and 27 water molecules was refined (Table 1) using data to 2.6 Å resolution with a free R value of 28.6% and a conventional R value of 25.2%.

The eag domain is an $\alpha + \beta$ protein with a five-stranded antiparallel β sheet (β A to β E) packed against a long ordered "vine" composed of coil and a single turn of 3_{10} helix (α 'A) (Figures 4A and 4B). The sheet is decorated on two sides by α helices (α A to α C). The

structure has its N and C termini positioned side by side forming the two central strands of the β sheet. Mass spectrometry confirmed that the crystals contain all 137 amino acids (the eag domain's 135 residues plus 2 residues from the fusion protein), indicating that the first 25 amino acids are disordered in the crystal. Additional (unmodelled) electron density is observed in both native and difference Fourier maps that might represent partially ordered segments of the missing N terminus. Interestingly, the disordered 25 N-terminal residues are among the most conserved in the eag domain (Warmke and Ganetzky, 1994). This conservation, together with the functional importance of the first 25 amino acids (see below) imply that this region may well be ordered in the context of the ion channel.

Mutational Analysis

In order to determine which eag domain residues establish the putative interface with the remainder of the HERG K⁺ channel, we produced 15 point mutations spread over the domain surface and measured their effect on function (Figures 5A and 5B). All point mutations were to alanine except for Arg-73, which was mutated to cysteine. The role of the disordered (within the crystal) N terminus was studied by producing three deletion mutants: deletion of residues 2 to 26 (Δ 2-26), 2 to 23 (Δ 2-23), and 2 to 9 (Δ 2-9). The effect of mutations was assessed by measuring the rate of deactivation as described above. The "speeding factor," defined as the ratio of time constants for the wild-type and mutant channels measured at -120 mV, is shown (Figure 5B). The mutants fall into three groups depending on the magnitude of effect. The largest group includes all mutations that have a speeding factor close to 1 (little or no

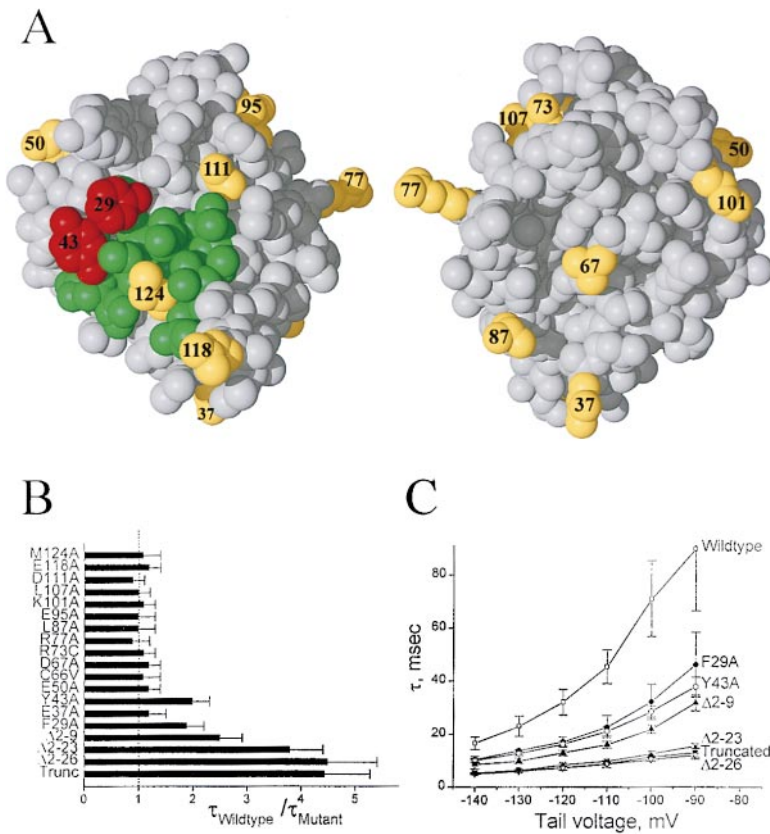


Figure 5. Mutational Analysis of the eag Domain

(A) Two views of a CPK model of the eag domain. The molecule is shown in the same orientation as in Figure 4 (right) and rotated by 180 degrees about a vertical axis (left). Mutated residues either affected (red; Phe-29 and Tyr-43) or did not affect (yellow) the deactivation rate. A hydrophobic patch is shown (green) and also includes Met-124, Phe-29, and Tyr-43. Picture drawn with BALLS (Merritt and Bacon, 1997).

(B) Bar plot of speeding factor (wild type-to-mutant time constant ratio) for deactivation at -120 mV. The dashed line marks a ratio of 1. Speeding factor for truncated HERG channels (Trunc) is also shown.

(C) Plot of deactivation time constant as a function of repolarization voltage for mutations that showed altered kinetics; data for wild-type and truncated HERG channels shown for comparison. Error bars are standard error of the mean ($n = 3 - 5$).

effect). A second group with a speeding factor close to 4 includes mutants Δ 2-26 and Δ 2-23, and a third with a factor around 2 includes F29A, Y43A, and Δ 2-9. Graphing the time constants over the full voltage range for the second and third groups (Figure 5C) shows that Δ 2-26 and Δ 2-23 are indistinguishable from truncated HERG, while the Δ 2-9 mutant channel is intermediate between wild-type and truncated HERG, as are mutants F29A and Y43A.

The two point mutations affecting deactivation (F29A and Y43A) are clustered on the domain surface (Figure 5A). Moreover, these functionally important amino acids are located within a hydrophobic patch having a solvent accessible area of 530 \AA^2 made up of residues Ile-31, Ile-42, Met-60, Val-113, Val-115, Ile-123, Met-124, and Ile-126, in addition to Phe-29 and Tyr-43. The functional importance of this patch is intriguing. In the crystal, the hydrophobic environment of the patch is maintained through packing of hydrophobic surfaces from two adjacent domains, resulting in a total buried surface area of 1190 \AA^2 (both sides of the interface). However, gel filtration and analytical ultracentrifugation show the eag domain to be a monomer (not shown). Given that the domain appears to be tightly adherent to the body of the K^+ channel, the hydrophobic patch may provide the interface through which it binds.

The functional importance of the very N terminus of the eag domain is interesting particularly in light of previous results of Terlau and colleagues (Terlau et al., 1997). They showed in a rat eag K^+ channel that deletion of amino acids 7 to 12 altered the rate of deactivation

and that the effect could be counteracted by a second mutation within the S4-S5 linker. The S4-S5 linker, that is, the connector between the fourth and fifth membrane-spanning segments, is a gating-sensitive region of voltage-dependent K^+ channels. Indeed, the S4 contains the basic amino acids underlying the voltage-dependent gate. We therefore speculate that when the eag domain is bound to the channel, the N-terminal amino acids are in a position to interact with residues in the S4-S5 linker. If this is the case, we might expect the N-terminal amino acids to become disordered when the eag domain is removed from the context of the channel.

The HERG N Terminus Is a Eukaryotic PAS Domain

The eag domain bears no structural resemblance to the tetramerization domain of the kV -type voltage-dependent K^+ channels (Kreusch et al., 1998), and in contrast to the tetramerization domain, the eag domain does not appear to self-oligomerize. The program DALI (Holm and Sander, 1994) was used to search the database for proteins with a three-dimensional structure similar to that of the eag domain. Photoactive yellow protein (PYP), a bacterial light-sensing protein, had a score three times higher than the next candidate, profilin. By aligning the β sheet of the two models (Figure 6A), it is clear that the eag domain and PYP have highly similar three-dimensional structures; the major difference between the two proteins occurs in the way the α C helix and associated "vine" pack against the β sheet. The rms deviation between the two structures for main chain atoms of residues marked by blue boxes in Figure 6B

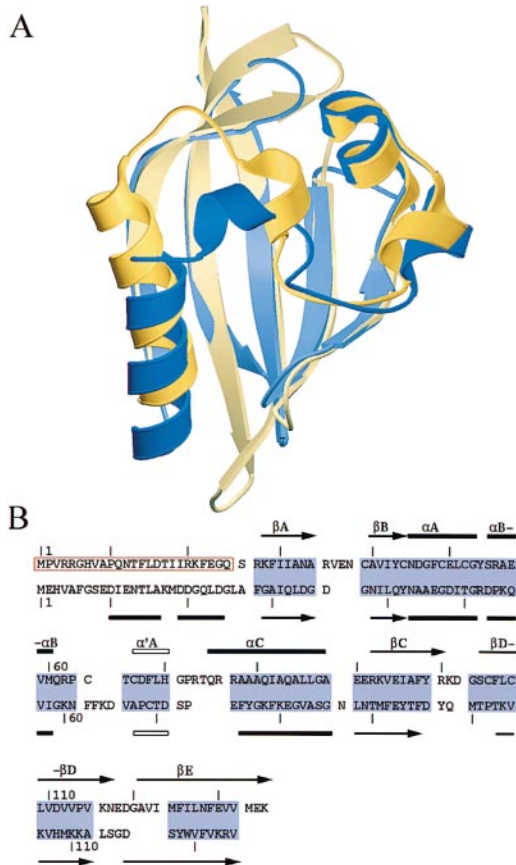


Figure 6. Structural Comparison of the eag Domain and Photoactive Yellow Protein (PYP)

(A) Ribbon diagram of superimposed eag domain (yellow) and PYP (blue) in same view as Figure 4.

(B) Sequence alignment of eag domain (top) and PYP according to the superimposed structures. The blue boxes mark stretches of sequence where aligned residues occupy the same position in secondary structure elements that are common to both structures. Secondary structural elements are marked above and below the corresponding sequence: α helices as arrows, β strands as filled rectangles, 3_{10} helix as open rectangle. The structural elements of the eag domain structure are labeled. The open red box marks residues that are disordered in the eag domain structure. Residue numbering is shown above and below the respective sequences.

is 2.5 Å; exclusion of residues corresponding to $\alpha'A$ and $\alpha'C$ drops this value to 1.4 Å. A structure-based sequence alignment of the eag domain and PYP shows that there is no significant sequence conservation (Figure 6B); the relatedness of these proteins is apparent only through comparison of their three-dimensional structures.

PYP belongs to the PAS domain family and until now was the only member with a known structure. These proteins are present in prokaryotes where they serve as sensory domains and in eukaryotes where they participate in the biochemical pathways underlying the circadian rhythm, among other functions. Due to extreme sequence diversity, only recently have the PAS domains been proposed as a broad protein family (Ponting and Aravind, 1997; Zhulin et al., 1997; Pellequer et al., 1998).

Table 1. Data and Refinement Statistics

Data and Phasing Quality			
Data Set (13.0–2.6/2.7–2.6 Å)	L1 (12.660 keV)	L2 (12.665 keV)	L3 (12.740 keV)
Completeness (%)	95.8/87.9	95.9/87.9	95.9/88.1
R_{merge}^a (%)	9.2/35.4	10.5/40.3	10.5/40.6
I/σ	34/5	32/4	33/4
Redundancy ^b	7/2.5	7/2.5	7/2.5
R_{cullis}^c (anomalous)	0.83	0.51	0.74
R_{cullis}^d (dispersive)	—	0.93	0.77
Overall FOM ^e	0.50		

Refinement Against L1 Data Set

Resolution	13.0–2.6 Å
$R_{\text{crystallographic}}^f$	25.2%
R_{free}^f	28.6%
Number of atoms	
Protein	817
Waters	27
No. of reflections with $F/\sigma F \geq 2$	3428
Rmsd ^g bond angles	0.833°
Rmsd ^g bond lengths	0.004 Å
Rmsd ^g B factor for bonded atoms	1.088 Å ²
Mean B factor for all atoms	33.2 Å ²

I is the average intensity, I_j is the observed intensity, D_{ph} is the observed anomalous difference, D_{phc} is the calculated anomalous difference, F_{ph} is the observed amplitude for the derivative, F_{p} is the observed amplitude for the native, F_{hc} is the calculated amplitude for the heavy atom, F_{pc} is the calculated native amplitude.

^a $R_{\text{merge}} = \sum \sum |I_j - I| / \sum I_j$.

^b Redundancy was calculated for separate Bijvoets pairs.

^c $R_{\text{cullis}}^{\text{anomalous}} = \sum |D_{\text{ph}} - D_{\text{phc}}| / \sum |D_{\text{ph}}|$ for acentric reflections.

^d $R_{\text{cullis}}^{\text{dispersive}} = \sum |F_{\text{ph}} - F_{\text{p}} + F_{\text{hc}}| / \sum |F_{\text{ph}} - F_{\text{p}}|$ for centric reflections.

^e FOM figure of merit.

^f $R_{\text{crystallographic}} = \sum |F_{\text{p}} - F_{\text{pc}}| / \sum |F_{\text{p}}|$; R_{free} the same, as $R_{\text{crystallographic}}$ but calculated on 14% of data excluded from refinement.

^g Rmsd, root-mean-square deviation.

Through this study, we have defined a eukaryotic PAS domain structurally.

Discussion

In prokaryotic cells, PAS domains appear to have a sensory function. For example, PYP is a photoreceptor involved in the negative phototaxis response to blue light in certain bacteria (Borgstahl et al., 1995; Genick et al., 1997). It has a chromophore (4-hydroxycinnamyl) covalently bound to a cysteine in the “vine” and buried in the core of the protein; upon absorption of a photon, the chromophore isomerizes, inducing a conformational change on the protein surface. This change is thought to initiate a signal transduction process that affects the motility system of the bacterium. An *E. coli* membrane protein called aerotaxis provides a second example (Bibikov et al., 1997; Rebbapragada et al., 1997). The cytoplasmic N terminus of this protein contains a PAS domain implicated in sensing redox potential; the cytoplasmic C terminus communicates with the flagellar motor.

In eukaryotic cells, the best known PAS domains are

found in proteins involved in the circadian rhythm (Repert, 1998; Sassone-Corsi, 1998). Monomeric forms of Per and Tim (*Drosophila* clock gene products) are localized to the cytosol, whereas heterodimerization, mediated by the PAS domain present in Per, leads to translocation to the nucleus where they exert a negative feedback control on their own expression. Another eukaryotic PAS domain is present in the aryl hydrocarbon receptor (dioxin receptor). In this system, the PAS domain is thought to be involved in both ligand binding as well as in a protein-protein interaction (Hahn et al., 1997).

HERG and other members of the eag K⁺ channel family contain a PAS domain on their cytoplasmic N terminus. Removal of this domain alters a physiologically important gating transition in HERG, and addition of isolated domain to the cytoplasm of cells expressing truncated HERG reconstitutes wild-type gating. Therefore, the domain finds the channel, attaches to it (presumably one domain per subunit through the hydrophobic patch on the domain surface), and confers its function. In summary, we conclude that the eag domain is a member of the PAS domain family and its role is to modify K⁺ channel gating. Further, given the regulatory roles of PAS domains in other protein systems, we suspect that the eag domain will have a dynamic influence on the gating of the HERG K⁺ channel through the binding of small molecule or protein effectors.

Experimental Procedures

Molecular Biology

The HERG channel was present in pSP64 vector between HindIII and BamHI sites. Mutations of the eag domain were generated by PCR mutagenesis across a HindIII/NcoI-flanked cassette; mutations were confirmed by automated sequencing. After DNA linearization with EcoRI, RNA was prepared by transcription with SP6 RNA polymerase.

Electrophysiology

Oocytes from *Xenopus laevis* were surgically removed and incubated for 1.5–2.5 hr in a solution containing: 1 mg/ml Collagenase type 2 (Worthington Biochemical Corporation), 82.5 mM NaCl, 2.5 mM KCl, 1.0 mM MgCl₂, 5.0 mM HEPES, pH adjusted to 7.6 with NaOH. Defolliculated oocytes (stages 5 and 6) were injected with cRNA encoding wild-type or mutant HERG channel and incubated for 12–24 hr in a solution containing: 50 μg/ml gentamycin (GIBCO), 96 mM NaCl, 2 mM KCl, 1.8 mM CaCl₂, 1.0 mM MgCl₂, 5.0 mM HEPES, pH adjusted to 7.6 with NaOH.

Whole cell recordings were performed using an OC-725A two-electrode voltage clamp (Warner Instruments); the data were filtered at 1 kHz. Microelectrode resistances were 0.3–2.0 MΩ when filled with 3 M KCl. The oocytes were studied under continuous perfusion with a solution containing 58 mM NaCl, 40 mM KCl, 0.3 mM CaCl₂, 1.0 mM MgCl₂, 5.0 mM HEPES, pH adjusted to 7.6 with NaOH. All experiments were carried out at room temperature. Measurements were rejected if the tail current peak was larger than 3.0 μA and if the voltage electrode drifted by more than 10 mV at the end of the experiment. Patch clamp experiments were performed using an Axopatch 200A (Axon Instruments) amplifier; the data were filtered at 1 kHz. The oocytes were studied in a two-well bath containing 140 mM KCl, 0.5 mM EDTA, 10 mM HEPES, pH adjusted to 7.6 with KOH, with the reference electrode separated from the oocyte bath by a salt bridge. Reconstitution experiments were performed with eag domain protein expressed and purified as described below. Before injection, the protein was dialyzed overnight against a solution containing 140 mM KCl, 0.5 mM EDTA, 10 mM HEPES, pH adjusted to 7.6 with KOH. Oocytes expressing truncated HERG

channel were injected with 100 nl of protein solution at a concentration of 70–90 μM.

Biochemistry

The eag domain (residues 1 to 135) was expressed as a glutathione-S-transferase (GST) fusion in *E. coli* BL21(DE3) strain after overnight induction at 20°C. Cells were lysed in the presence of 0.1% Tween-20 (Pierce). The lysate was mixed with glutathione-Sepharose (Pharmacia), and the protein was eluted after thrombin digestion in a buffer containing 10 mM dithiothreitol (DTT) and 5 mM n-octyl-β-D-glucoside (Anatrace). Further purification was carried out by gel filtration in a Sephadex75 (Pharmacia) column equilibrated in a buffer containing 1 mM DTT without detergent. Final concentration was done in the presence of 10 mM DTT and 5 mM n-octyl-β-D-glucoside (analytical grade). Selenomethionine substituted protein was expressed and purified as described above with the following changes: B834(De3) *E. coli* strain, minimal media supplemented with essential amino acids except for methionine, which was substituted with selenomethionine. Mass spectrometry (MALDI-TOF) (Chait, 1994) was carried out to confirm that protein crystals were formed with full-length polypeptide and that full selenomethionine substitution occurred. Analytical centrifugation was performed in a Beckman Optima XL-A at three protein concentrations in 50 mM Tris (pH 8.0), 150 mM NaCl, 5 mM n-octyl-β-D-glucoside, 1 mM DTT.

Crystallization and Crystallographic Methods

Crystals were grown at 20°C by sitting-drop vapor diffusion. Protein solution at ~10 mg/ml in 10 mM DTT, 5 mM n-octyl-β-D-glucoside, 150 mM NaCl, 50 mM Tris (pH 8.0) was mixed with an equal volume of reservoir solution: 0.8–1.0 M sodium and potassium tartrate, 100 mM HEPES (pH 7.0). The eag domain was crystallized in spacegroup P6₃22, with cell dimensions a = 56.1 Å, c = 135.5 Å and one molecule in the asymmetric unit. The crystals were difficult to reproduce and suffered from nonisomorphism, making heavy-atom search a difficult task. All diffraction data for the MAD (multiwavelength anomalous diffraction) experiment were collected on a single selenomethionine-substituted protein crystal at Cornell High Energy Synchrotron Source (CHESS) at F2 station on a ADSC Quantum-4 CCD camera. Some native data were also collected at X12-C station at the National Synchrotron Light Source. Crystals were flash-frozen in freshly thawed liquid propane after being cryoprotected in crystallization solution containing increasing amounts of glycerol (5%–20%). After wavelength calibration and fluorescence scan of a wet-mounted crystal, six data sets were collected with inverted beam geometry at three energies (inflection point, 12.660 keV; peak, 12.665 keV; and remote, 12.740 keV). Data were integrated with DENZO, and scaling was performed in SCALEPACK (Otwinowski, 1993) in two steps. First, scale and B factors were calculated simultaneously for all data images. These factors were then used for internal scaling of each wavelength data set. Further processing was done with the CCP4 package (CCP4, 1994). SHELX (Sheldrick, 1990) was used to determine the position of the first selenium by direct methods and Patterson search. Initial phases were calculated in MLPHARE (CCP4, 1994), and two more selenium positions were confirmed on difference maps. Phases were calculated in MLPHARE using the inflection point data set as the native reference (Table 1). After solvent-flattening in DM (Cowtan, 1994), an electron density map of excellent quality was calculated that permitted the tracing of most of the model. Refinement (Table 1) consisted of rounds of model building in the program O (Jones et al., 1991) followed by bulk solvent correction, positional refinement (phase restraints were included in some of the cycles), and restrained B factor refinement with X-PLOR (Brunger, 1996). Electron density difference maps confirmed the presence of unaccounted density in the native map; this density might be attributed to the disordered N terminus. The final model includes residues 26 to 135 and 27 water molecules. The following side chains have been truncated: Ser-26 to C_α, Arg-35 to C_γ, Glu-37 to C_β, Gln-75 to C_δ, Arg-76 to C_β, Arg-77 to C_β, Gln-84 to C_β, Glu-90 to C_β, Glu-118 to C_β, Asp-119 to C_α, and Glu-130 to C_γ. According to PROCHECK (CCP4, 1994) 89.8% of the main chain torsional angles are in the most favored regions of the Ramachandran plot and none in the generously allowed or disallowed areas.

Acknowledgments

We thank D. Thiel, S. Gruner, and members of the MacCHESS staff for support and assistance in data collection at F2; J. Imredy for many helpful discussions and technical advice; Y. Jiang and D. Doyle for help with data collection; and S. Mann and K. Loeffert for help with protein expression. This research was funded by NIH GM47400 (to R. M.) and NIH RR00862 (to B. T. C.) and NIH NS33324 (to M. L.). M. L. is an A. H. A. Pfizer awardee. R. M. is an investigator of the Howard Hughes Medical Institute.

Received August 17, 1998; revised September 23, 1998.

References

- Bacon, D., and Anderson, W.F. (1988). A fast algorithm for rendering space-filling molecule pictures. *J. Mol. Graph.* **6**, 219–220.
- Bibikov, S.I., Biran, R., Rudd, K.E., and Parkinson, J.S. (1997). A signal transducer for aerotaxis in *Escherichia coli*. *J. Bacteriol.* **179**, 4075–4079.
- Borgstahl, G.E.O., Williams, D.R., and Getzoff, E.D. (1995). 1.4 Å structure of photoactive yellow protein, a cytosolic photoreceptor: unusual fold, active site and chromophore. *Biochemistry* **34**, 6278–6287.
- Brunger, A.T. (1996). X-PLOR (version 3.851) Manual. (The Howard Hughes Medical Institute and Department of Molecular Biophysics and Biochemistry, Yale University, New Haven, CT).
- CCP4, Collaborative computational project 4 (1994). The CCP4 suite: programs for protein crystallography. *Acta Crystallogr.* **D50**, 760–763.
- Chait, B.T. (1994). Mass-spectrometry — a useful tool for the protein X-ray crystallographer and NMR spectroscopist. *Structure* **2**, 465–467.
- Cowan, K. (1994). DM: an automated procedure for phase improvement by density modification. Joint CCP4 and ESF-EACBM Newsletter on Protein Crystallography **31**, 34–38.
- Curran, M.E., Splawski, I., Timothy, K.W., Vincent, G.M., Green, E.D., and Keating, M.T. (1995). A molecular basis for cardiac arrhythmia: HERG mutations cause long QT syndrome. *Cell* **80**, 795–803.
- Genick, U.K., Borgstahl, G.E.O., Ng, K., Ren, Z., Pradervand, C., Burke, P.M., Srajer, V., Teng, T.-Y., Schidkamp, W., McRee, D.E., Moffat, K., and Getzoff, E.D. (1997). Structure of a protein photocycle intermediate by millisecond time-resolved crystallography. *Science* **275**, 1471–1475.
- Hahn, M.E., Karchner, S.I., Shapiro, M.A., and Perera, S.A. (1997). Molecular evolution of two vertebrate aryl hydrocarbon (dioxin) receptors (AHR1 and AHR2) and the PAS family. *Proc. Natl. Acad. Sci. USA* **94**, 13743–13748.
- Holm, L., and Sander, C. (1994). The FSSP data base of structurally aligned protein fold families. *Nucleic Acids Res.* **22**, 3600–3609.
- Jones, T.A., Zou, J.Y., Cowan, S., and Kjeldgaard, M. (1991). Improved methods for building protein models in electron density maps and the location of errors in the models. *Acta Crystallogr.* **A47**, 110–119.
- Kraulis, P. (1991). MOLSCRIPT: a program to produce both detailed and schematic plots of protein structures. *J. Appl. Cryst.* **24**, 946–950.
- Kreusch, A., Pfaffinger, P.J., Stevens, C.F., and Choe, S. (1998). Crystal structure of the tetramerization domain of the Shaker potassium channel. *Nature* **392**, 945–948.
- Li, X., Xu, J., and Li, M. (1997). The human $\Delta 1261$ mutation of the HERG potassium channel results in a truncated protein that contains a subunit interaction domain and decreases the channel expression. *J. Biol. Chem.* **272**, 705–708.
- Merritt, E.A., and Bacon, D.J. (1997). RASTER3D: photorealistic molecular graphics. *Methods Enzymol.* **277**, 505–524.
- Otwinowski, Z. (1993). Oscillation data reduction program. In *Data Collection and Processing*, L.Sawyer, N.Isaacs, and S. Bailey, eds. (Daresbury Laboratory, Daresbury, UK: Science and Engineering Research Council), pp. 56–62.
- Pellequer, J.-L., Wager-Smith, K.A., Kay, S.A., and Getzoff, E.D. (1998). Photoactive yellow protein: a structural prototype for the three-dimensional fold of the PAS domain superfamily. *Proc. Natl. Acad. Sci. USA* **95**, 5884–5890.
- Ponting, C.P., and Aravind, L. (1997). PAS: a multifunctional domain family comes to light. *Curr. Biol.* **7**, R674–R677.
- Rebbapragada, A., Johnson, M.S., Harding, G.P., Zuccarelli, A.J., Fletcher, H.M., Zhulin, I., and Taylor, B.L. (1997). The AER protein and the serine chemoreceptor TSR independently sense intracellular energy levels and transduce oxygen, redox and energy signals for *Escherichia coli*. *Proc. Natl. Acad. Sci. USA* **94**, 10541–10546.
- Reppert, S.M. (1998). A clockwork explosion! *Cell* **21**, 1–4.
- Sanguinetti, M.C., Jiang, C., Curran, M.E., and Keating, M.T. (1995). A mechanistic link between an inherited and an acquired cardiac arrhythmia: HERG encodes the I_{Kr} potassium channel. *Cell* **81**, 299–307.
- Sassone-Corsi, P. (1998). Molecular clocks: mastering time by gene regulation. *Nature* **392**, 871–874.
- Schonherr, R., and Heinemann, S.H. (1996). Molecular determinants for activation and inactivation of HERG, a human inward rectifier potassium channel. *J. Physiol.* **493**, 635–642.
- Sigworth, F.J. (1994). Voltage gating of ion channels. *Q. Rev. Biophys.* **27**, 1–40.
- Sheldrick, G.M. (1990). Phase annealing in SHELX-90: direct methods for larger structures. *Acta Crystallogr.* **46**, 467–473.
- Smith, P.L., Baukowitz, T., and Yellen, G. (1996). The inward rectification mechanism of the HERG cardiac potassium channel. *Nature* **379**, 833–836.
- Spector, P.S., Curran, M.E., Zou, A., Keating, M.T., and Sanguinetti, M.C. (1996). Fast inactivation causes rectification of the I_{Kr} channel. *J. Gen. Physiol.* **107**, 611–619.
- Terlau, H., Heinemann, S.H., Stühmer, W., Pongs, O., and Ludwig, J. (1997). Amino terminal-dependent gating of the potassium channel rat eag is compensated by a mutation in the S4 segment. *J. Physiol.* **502**, 537–543.
- Trudeau, M.C., Warmke, J.W., Ganetzky, B., and Robertson, G.A. (1995). HERG, a human inward rectifier in the voltage-gated potassium channel family. *Science* **269**, 92–95.
- Warmke, J.W., and Ganetzky, B. (1994). A family of potassium channel genes related to *eag* in *Drosophila* and mammals. *Proc. Natl. Acad. Sci. USA* **91**, 3438–3442.
- Warmke, J.W., Drysdale, R., and Ganetzky, B. (1991). A distinct potassium channel polypeptide by the *Drosophila eag* locus. *Science* **252**, 1560–1562.
- Zhulin, I.B., Taylor, B.L., and Dixon, R. (1997). PAS domain S-boxes in Archae, Bacteria and sensors for oxygen and redox. *Trends Biochem. Sci.* **22**, 331–333.

Brookhaven Protein Data Bank ID Code

Coordinates of the refined HERG potassium channel PAS domain have been deposited in the Protein Data Bank (Brookhaven Laboratory) with ID code 1byw.